# Experimental Study of Catalytic Slow Pyrolysis of Palm Shell: Product Characteristic, Possible Mechanism, and Valuable Chemicals

Joko Pitoyo*, Siti Jamilatun*‡, Totok Eka Suharto*

*Department of Chemical Engineering, Faculty of Industrial Technology, Universitas Ahmad Dahlan, Jl. Jend. Ahmad Yani, Banguntapan, Bantul, Yogyakarta, Indonesia 55166

(joko2107054001@webmail.uad.ac.id, sitijamilatun@che.uad.ac.id, totok.suharto@che.uad.ac.id)

‡ Corresponding Author; Siti Jamilatun, Department of Chemical Engineering, Faculty of Industrial Technology, Universitas Ahmad Dahlan, Tel: +62 813-2915-7053, sitijamilatun@che.uad.ac.id

*Received: 09.12.2023 Accepted:30.01.2024*

**Abstract-** Palm shell is one of Indonesia's most significant agricultural products, as well as the waste it produces. Pyrolysis is the most effective method for converting biomass into biofuel and valuable chemicals. Understanding the decomposition mechanism of pyrolysis is crucial for reactor design and optimization. This research aims to study the characteristics of palm shell pyrolysis products, possible reaction mechanisms, and resulting valuable compounds. Palm shell slow pyrolysis at a heating rate of 10 °C/min was performed in a fixed-bed reactor using Ni/$Al_2O_3$ catalyst 20 wt.% at 300, 400, 500, and 600°C. The result shows that the optimum yield of bio-oil was obtained at a temperature of 500 °C. The catalyst increased the heating value and decreased the oxygenated and O/C content of bio-oil. Ni/$Al_2O_3$ catalyst has high selectivity to phenol, aliphatic hydrocarbon, and aldehyde. The biochar product has a microporous structure with a mean pore diameter of 1.89 nm and a surface area of 0.3899 $m^2$/g. Ni/$Al_2O_3$ catalyst is effective for reforming process shown by decreasing $CH_4$ and $CO_2$ content. The phenolic component is the foremost valuable chemical in palm shell pyrolysis.

**Keywords** Palm shell, pyrolysis, nickel alumina, biofuel, valuable chemicals.

## 1. Introduction

In 2022, Indonesia is expected to generate 45.58 million tons of palm oil; according to the Central Statistics Agency (BPS), looking at the trend, Indonesia's production of palm oil has an upward tendency [1]. The amount of palm waste produced in Indonesia rises in correlation with the country's growing production of palm oil, including palm shells, palm sludge, empty palm fruit bunches, liquid waste, and fibers [2]. The processing of fresh fruit bunches from oil palm produces 6.5% of palm shells [3].

Biochemical and thermochemical are the two main methods for converting biomass into biofuel [4]. The former includes fermentation, hydrolysis, extraction [5], and anaerobic digestion [6]. Combustion, pyrolysis, and gasification are examples of the latter [7]. Pyrolysis is a heat-assisted decomposition process without the use of oxidizing agents [8]–[10]. It is regarded as an effective method compared to other thermochemical conversions because of its broader operating temperature range (300-600 °C), ability to operate at standard pressure, and capacity to simultaneously produce three value-added products (liquid, gas, and solid) [11]–[13].

The pyrolysis of palm shells has been the subject of many research studies, including upgrading methods, operating parameters, and reactor configuration [14]–[16]. Niu et al. performed in-situ flash pyrolysis of palm shells using HZSM-5 catalyst in the py-GCMS and py-PIMS reactors [17]. Kim et al. performed palm shell pyrolysis using Alumina, ZSM-5, and eq. FCC catalyst in a fluidized bed reactor [18]. The reaction mechanism and the resulting value-added chemicals, especially for palm shell pyrolysis, are rarely studied. Lack of understanding of reaction mechanisms and resulting valuable chemicals will have an impact on the difficulty of process design and optimization and will hinder further exploration of the potential of pyrolysis products, respectively. In this study,

we conducted palm shells' slow pyrolysis using $Ni/Al_2O_3$ in a fixed bed reactor with a simultaneous ex-situ process (pyrolysis and upgrading were carried out in one reactor, consisting of two cylinders (R1 and R2) arranged vertically in series) and then characterized the resulting product. This research aims to study product characteristics, possible decomposition mechanisms, and the resulting valuable chemicals. Knowledge of product characteristics leads to determining the possible reaction mechanism that occurs and the valuable chemicals produced. This finding will add specific information related to the pyrolysis of lignocellulosic biomass by showing the reaction mechanism and potential products of the pyrolysis process, especially lignocellulosic biomass with high lignin content.

## 2. Materials and Methods

### *2.1. Preparation of Palm Shell*

Palm shell was obtained from PTPN V, Riau. The sample was washed and followed by a drying process at 105 °C for 24 hours. The sample was then ground and screened to produce grain sizes of 0.425-2.00 mm. Table 1 presents the findings of the ultimate analysis from this study and also the compositional and proximate analyses from the literature [14], [19].

**Table 1.** Phsyco-chemical properties of palm shells

| Proximate (wt.%) | | Ultimate (wt.%) | |
|---|---|---|---|
| Moisture content | 11 | C | 48.99 |
| Fixed carbon | 19.7 | H | 6.6 |
| Volatile matter | 67.2 | N | 0.37 |
| Ash | 2.1 | S | 0.076 |
| Composition (wt.%) | | O | 43.96 |
| Cellulose | 27.7 | O/C | 0.67 |
| Hemicellulose | 21.6 | H/C | 1.62 |
| Lignin | 44 | HHV (MJ/Kg) | 24.27 |

### *2.2. Preparation of Catalyst*

$Ni/Al_2O_3$ catalyst was received from PT Pupuk Kujang Jawa Barat in pellet form. A hammer mill was used for crushing the catalyst. The crushed catalyst was stolen for a 0.42- to 2.00 mm grain size.

### *2.3. Catalytic Pyrolysis*

A fixed bed reactor with a height of 600 mm, an inside diameter of 400 mm, and an outside diameter of 440 mm was used to conduct the investigation. The reactor had an electric heater made of nickel wire that was spirally coiled around the reactor's exterior. The reactor temperature was determined using a thermocouple, and a 0.5 kva TGDC regulator was used to control the heating rate. There are two vertical cylinders in the reactor. The first cylinder (R1) was used for the palm shell, while the second (R2) was for catalysts. The catalyst-containing portion of R2 received the gas product from R1 and directed it upward and then downward to the condenser. The experiment setup can be seen in Figure 1.

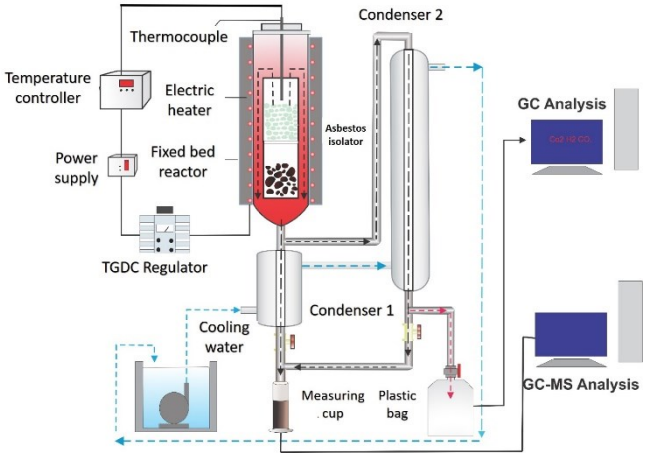


**Fig. 1.** Experimental setup of palm shell pyrolysis.

Catalytic pyrolysis was conducted by inserting a 50 g sample into R1 and 40 wt.% catalyst into R2, while non-catalytic pyrolysis was conducted without catalyst. The sample was heated to the expected temperature of 300, 400, 500, or 600 °C at a heating rate of 10 °C/minute. Once the temperature reached the required level, the heating continued isothermally for 15 min. The tar product was gathered in a measuring cup, weighed, and analyzed using GC-MS. The charcoal was taken at the end of pyrolysis and then weighed and analyzed using BET-BJH. Once gathered, the gas product was placed in a plastic container, and its content was analyzed using GC-TCD.

### *2.4. Product Analysis*

The component identification of the bio-oil was carried out using Gas Chromatography-Mass Spectrometry (Shimadzu, QP2010-SE). Surface characteristics of biochar were analyzed using Gas Sorption Analyzer (Quantachrome Novatouch LX-4) with a Full isothermal-40pts parameter. Analysis was performed using the $N_2$ adsorption-desorption method at a degassing temperature of 300 °C within 1 hour. The gas from the pyrolysis process was analyzed using a Shimadzu 8A Gas Chromatograph.

## 3. Result and Discussion

### *3.1. Characteristics of Palm Shell Thermal Decomposition*

Figure 2 shows the mass evolution of palm shell decomposition. The figure reveals that the initial mass loss of palm shells occurs between 190 and 200 °C. Due to the complexity of the palm shell constituent, a large temperature range (between 190 and 600 °C) is required for its thermal decomposition. At stage I, the temperature range for the decomposition is between 190 and 300 °C. The mass evolution curve at stage 1 shows a mass reduction of 15%. The

decomposition of the palm shell at this stage caused by the hemicellulose decomposition. The primary decomposition occurred at the range of 300 to 420 °C (stage II), with 365 °C being the maximum decomposition temperature. At this stage, hemicellulose, cellulose, and lignin were all decomposing simultaneously, with cellulose decomposition acting as a primary decomposition [20]. The temperature decomposition of hemicellulose occurs between 250 and 350 °C, cellulose at the range of 325 to 400 °C, and lignin at the range of 300-550 °C. The slow decomposition rate at stage III may be caused by the lignin and secondary biochar decomposition [21], [22]. Figure 2 presents that the derivative mass curve shows the existence of one shoulder, one peak, and the likelihood of forming a second peak at 600 °C related to the hemicellulose, cellulose, and lignin decomposition, respectively [20].

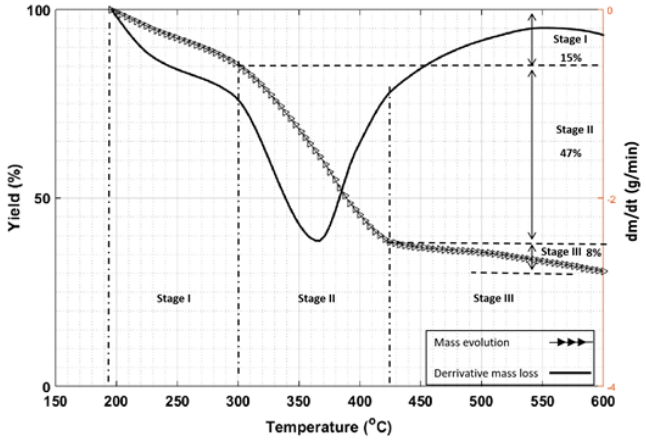


**Fig. 2.** Thermal decomposition interpolated curve of palm shell pyrolysis.

### *3.2. Characteristic of Tar Product*

The tar consists of bio-oil and water phases. Figure 3 shows the yield at various experimental temperatures, including catalytic and non-catalytic pyrolysis. The optimal bio-oil yield was obtained at 500 °C for catalytic and non-catalytic pyrolysis with yields of 10.47% and 13.02%, respectively. The yield of bio-oil increases along the temperature of 300 to 500 °C. Increasing the temperatures over 500 °C decreases the yield due to the secondary tar decomposition that promotes the forming of non-condensable gas. It can be seen that using a catalyst decreases the bio-oil yield by an average of 2.82%. This occurs because using a catalyst promotes the secondary decomposition of tar via cracking, decarbonylation, decarboxylation, hydrocracking, hydrodeoxygenation, and hydrogenation. Catalytic pyrolysis produces a lower yield of the water phase. This occurs because the catalyst will increase the water gas shift reaction that produces hydrogen ($H_2$) and carbon monoxide ($CO_2$) and improve the reforming process, which converts $H_2O$ into $H_2$ gas [23]–[25].

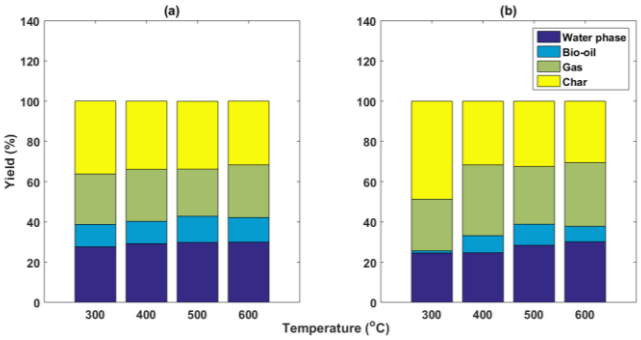


**Fig. 3.** Yields of pyrolysis product at different pyrolysis temperatures for a) non-catalytic pyrolysis and b) catalytic pyrolysis.

Figure 4 reveals that phenolic components (phenol and substituted phenol) and acids in the form of long-chain fatty acids (LCFA) are the primary components in the palm shell bio-oil. Phenol is the most significant phenolic component, with an average percentage of 65.21% and 45.44% for catalytic pyrolysis and non-catalytic, respectively. The LCFA comprises fatty acids with a chain length of C atoms between 12 and 18, such as oleic acid, palmitic acid, lauric acid, myristic acid, and potentially crude biodiesel. In the case of non-catalytic pyrolysis, fatty acid formation rose from 300 to 400 °C and subsequently somewhat decreased above 400 °C. The degradation of both cellulose and hemicellulose causes this rising of fatty acid through the depolymerization of oligosaccharides into xylose, which then decomposes further to form acids, furfural, and furan. Likewise, it occurs due to the dehydration of hydroxyl aldehydes, which become aldehydes such as furan, which are then further hydrated to become acids [26]. This could also occur due to breaking the branch chain of ferulic acid ester in xylan to carboxylic acids [27]–[30]. Meanwhile, the decrease in fatty acid content was due to the decarboxylation of fatty acids into aliphatic and aromatic hydrocarbons.

Using $Ni/Al_2O_3$ catalyst increased the formation of phenol components with an average increase of 20% and reduced the content of phenolic components (phenol complex/substituted phenol). This is due to the possibility that using a catalyst increases the polymerization of unsaturated light elements such as propylene, butane, and butadiene via gas-phase polymerization [31]. Breaking the branch chain of ferulic acid ester in xylan through decarboxylation produces vinyl guaiacol, which is further decomposed to produce guaiacol through hydrogenation, which then undergoes further decomposition to produce phenol [29]. Another factor that causes an increase in the phenol content in catalytic pyrolysis is the increase of the iso-substitution (radical-induced rearrangement) reaction of guaiacol and syringe, which produces cresol and xylenol and then further decomposed through demethylation reaction to produce phenol [30].

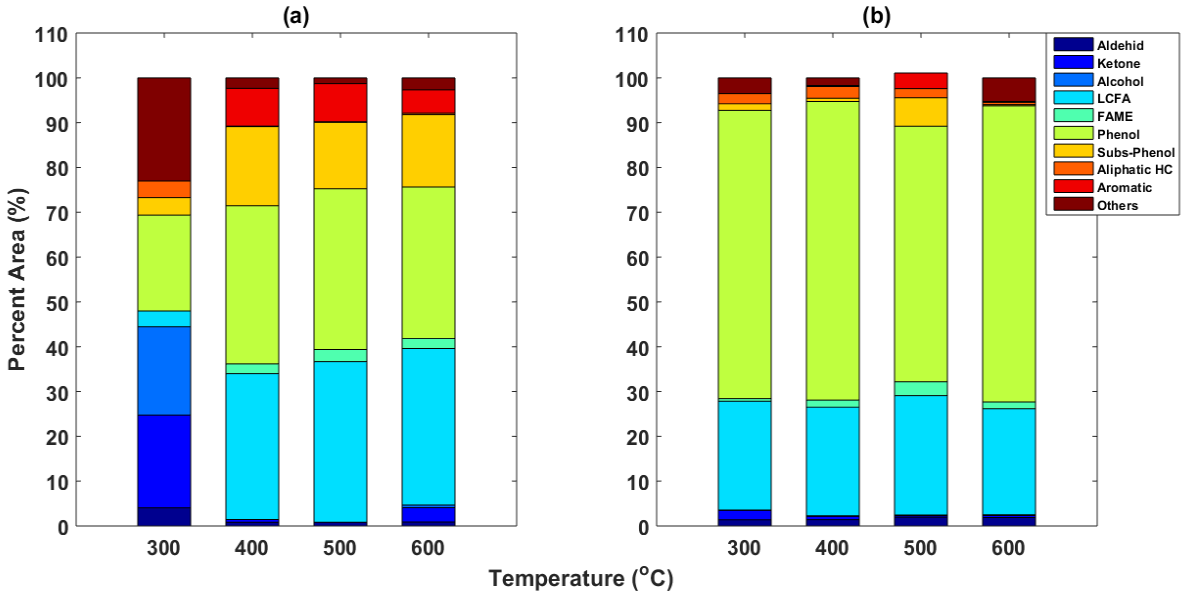


**Fig. 4.** Pyrolysis product compositions at different pyrolysis temperatures for a) non-catalytic pyrolysis and b) catalytic pyrolysis.

Figure 1 presents bio-oil chromatogram at different pyrolysis temperatures. The chromatogram of non-catalytic pyrolysis bio-oil has six dominant compounds: aldehydes, ketones, phenolics, aromatics, acids, and esters. For catalytic pyrolysis, there are six dominant groups of compounds: aldehydes, ketones, phenolics, hydrocarbons, acids (acids), and esters. In the chromatogram of non-catalytic pyrolysis, the phenolic and aromatic components have a longer retention time than in catalytic pyrolysis, which indicates that the catalyst can reduce the amount (variant) of the phenolic and aromatic components. In contrast, the hydrocarbon components in the chromatogram of catalytic pyrolysis had a longer retention time, indicating an increase in the number (variant) of the hydrocarbon components.

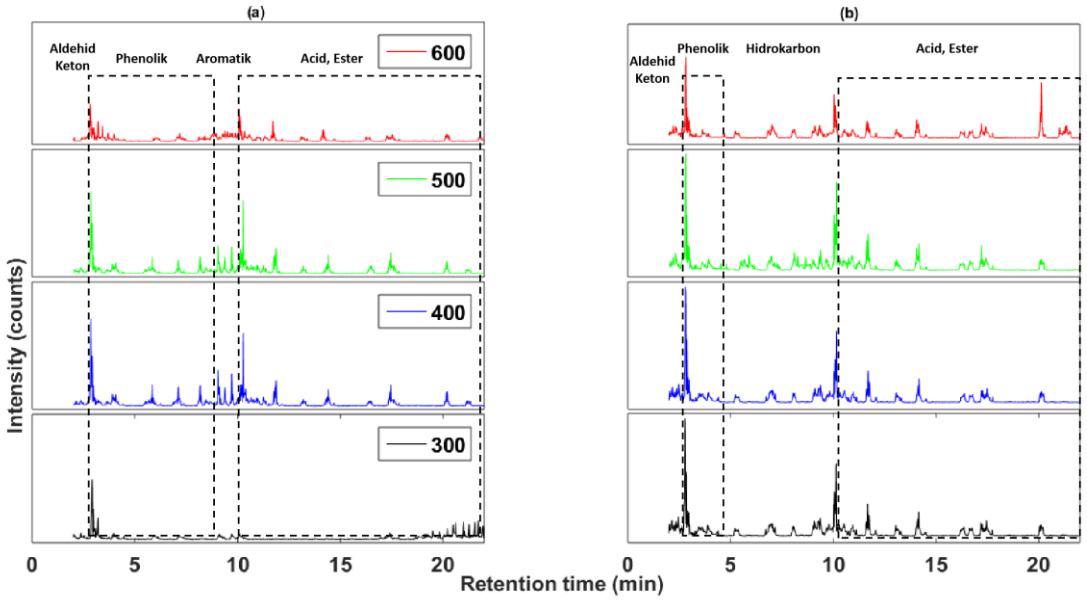


**Fig. 5.** Bio-oil chromatogram at different pyrolysis temperatures: a) non-catalytic, b) catalytic.

Figure 6 compares bio-oil functional groups between catalytic and non-catalytic pyrolysis. In general, the use of $Ni/Al_2O_3$ catalyst decreases the yield of ketones, furans, alcohols, carboxylic acids/fatty acid (LCFA), phenol complexes, and aromatic compounds and increases the yield of phenols, aliphatic hydrocarbons, aldehydes, and ester. The decrease in alcohol content is due to the hydrodeoxygenation of alcohol into aliphatic hydrocarbons. The decline in ketone content is probably due to the decarbonylation of ketones into aliphatic hydrocarbons. The decrease in furan content is caused by oligomerization, decarbonylation, and decarboxylation to produce a hydrocarbon pool or coke.

Meanwhile, the decrease in fatty acid content was caused by a decarboxylation reaction, which produced aliphatic hydrocarbons with C chain lengths between 12 and 18, and by

a reduction reaction, which had aldehyde. Demethylation and demethoxylation of phenol complexes (substituted phenol) such as guaiacol, syringol, and xylenol increase the formation of phenol. The increase in aliphatic hydrocarbon content is caused by decarbonylation, decarboxylation, and hydrodeoxygenation reactions. The reduction in the aromatic hydrocarbon and aliphatic hydrocarbon content at high temperatures may be caused by the cracking of the components into light hydrocarbons or coke formation. The explanation above showed that the $Ni/Al_2O_3$ catalyst was selective for constructing phenols, aliphatic hydrocarbons, and aldehyde. The possible decomposition mechanism for pyrolysis of palm shells using a $Ni/Al_2O_3$ catalyst can be seen in Figure 7.

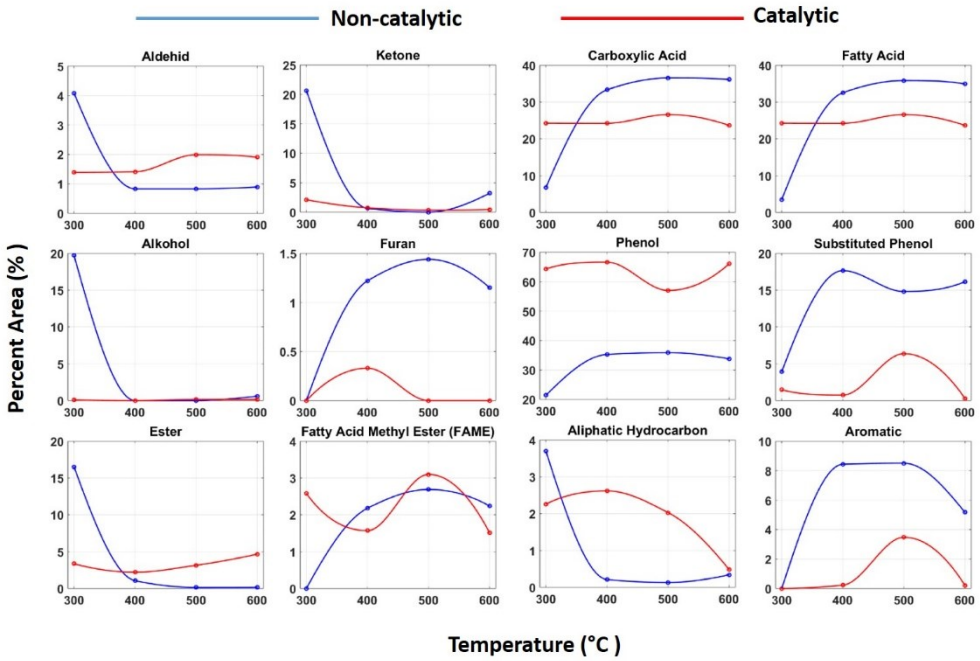


**Fig. 6.** Comparison of the functional group between non-catalytic and catalytic pyrolysis.

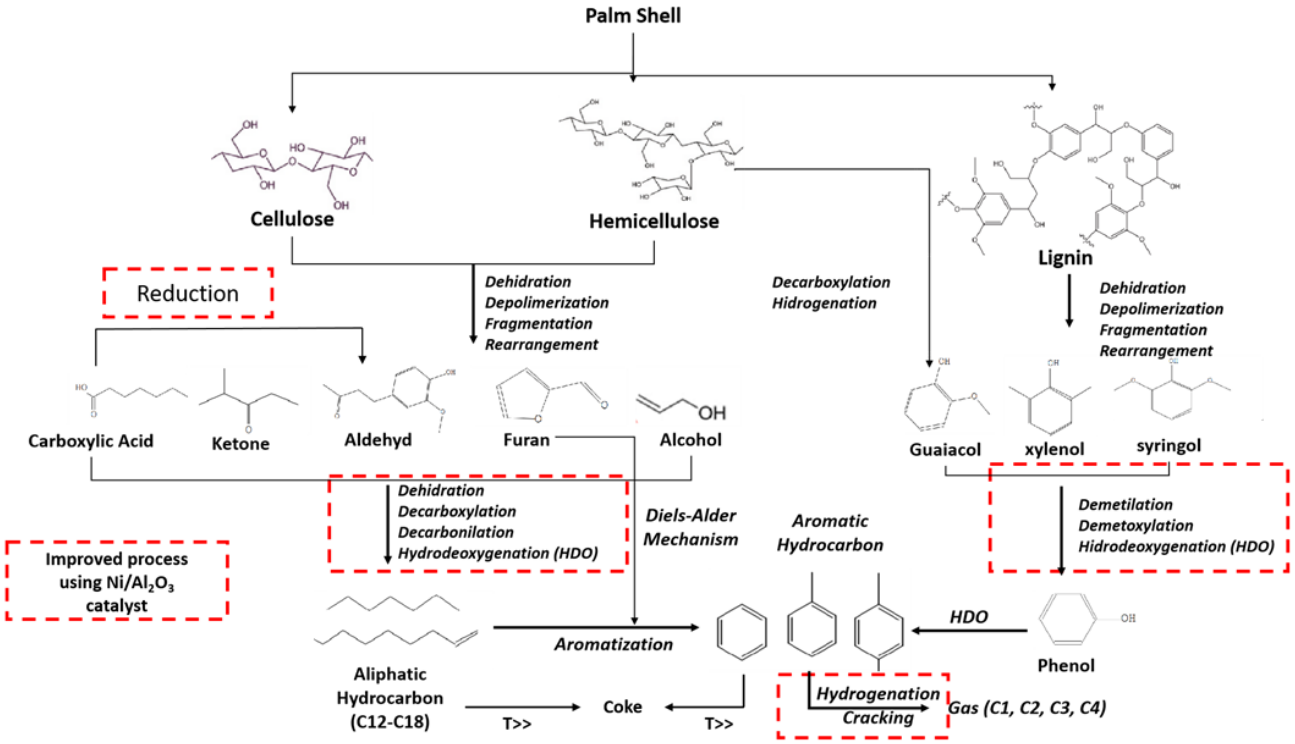


**Fig. 7.** Possible mechanism of palm shell pyrolysis using Ni/Al2O3.

Figure 8 shows that increasing temperature does not have a significant impact on improving HHV, decreasing O/C, and reducing oxygenate content. Meanwhile, the use of $Ni/Al_2O_3$ catalysts can have a significant effect on increasing HHV, decreasing O/C, and reducing oxygenate content. Hu et al. stated that the Ni catalyst had a high selectivity for the hydrodeoxygenation of oxygenate compounds [32]. Reducing the oxygenate content will decrease the O/C value and increase the HHV value. Using a $Ni/Al_2O_3$ catalyst can increase the cracking of oxygenic compounds, including carboxylic acids, to produce aliphatic hydrocarbons [33]. Using a $Ni/Al_2O_3$ catalyst will increase the hydrogenation reaction, which causes oxygen removal through internal dehydration and decarboxylation during the initial step of pyrolysis [34]. Likewise, the existence of Ni catalyst will increase the reforming process between oxygenated hydrocarbons, and the water content in bio-oil produces $CO_2$ through the aqueous reforming process (ARP) [35].

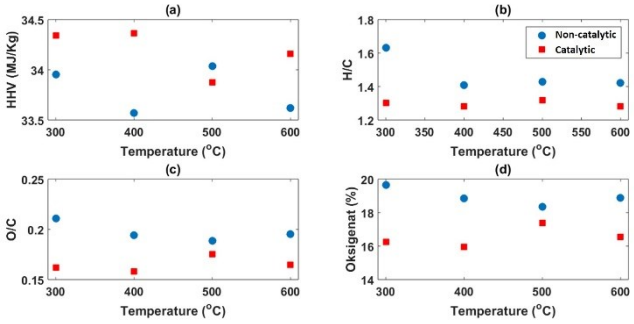


**Fig. 8.** HHV, H/C, O/C, and oxygenated value of obtained bio-oil at different temperature.

Palm shell bio-oil from palm shell contains value-added chemicals in phenolic components, including phenol, syringe, guaiacol, creosol, and eugenol. The phenolic part comes from lignin decomposition [15], [36]. Figure 9 shows the phenol and substituted phenol component in the palm shell bio-oil.

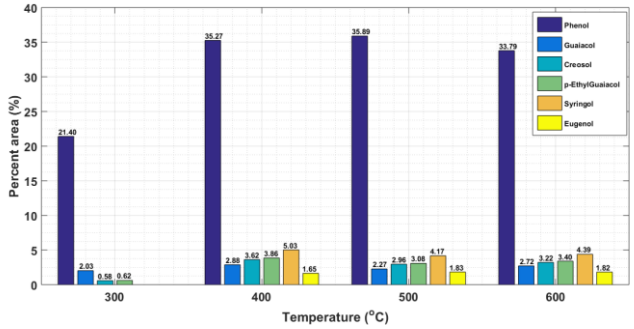


**Fig. 9.** Valuable chemicals from palm shell pyrolysis.

Figure 9 shows that phenol, as a major constituent of the bio-oil, has a value of 21.40-35.89 %. Phenol is the basic material of many chemical industries such as bio-plastics, epoxy resins, phenolic resins, polyurethanes, antimicrobial agents [15], and other applications [36], [37]. The bio-oil also contains guaiacol in the range of 2.03-2.88 %. Guaiacol is a guaiacum derivate and is found in various essential oils. Guaiacol acts as an aromatic oil and beneficial precursor for green fuel production. Guaiacol and syringol are the significant products of hardwood lignin pyrolysis [38]. Eugenol is included in the phenylpropanoid group of phenolic components and is the major constituent of clove oil. Eugenol exhibits a range of pharmacological activities such as antimicrobial, antioxidant, analgesic, anti-inflammatory, and local anesthetic [39]. Apart from having wide applications in the food, pharmaceutical, cosmetic, and industrial fields, the pyrolysis product also has an attractive price, as shown in Table 2. It makes the refinery process of valuable chemicals still promising.

**Table 2.** Valuable chemicals obtained from palm shell pyrolysis

| Component | Application | Price ($) |
|---|---|---|
| Phenol | Antimicrobial, phenolic resin, multiplex, pharmaceutical [36], [40] | 120,57/100 g |
| Guaiacol | Anticancer [41], antimicrobial [42], vanillin manufacturing [43] | 13,52/100 g |
| p-Ethylguaiacol | Fragrances, antioxidants [44] | 166,57/100 g |
| Creosol | Flavoring agents, biofuels [45] | 74,57/ml |
| Syringol | Flavoring agents, fragrances [46] | 106,28/100 g |
| Eugenol | Inhibits campylobacter activity [47], [35], inflammatory response inhibitor [39] | 24,00/100 mg |

### *3.3. Characteristics of Biochar Product*

In addition to producing bio-oil, pyrolysis also produces biochar [48]. Biochar can be used as a catalyst , adsorbent [49], carbon electrode, magnetic for waste remediation, or supercapacitor [50]. Figure 10 shows the results of BET and BJH analysis of biochar at the 550 °C pyrolysis temperature. Figure 10a shows that based on the IUPAC classification and according to the type of adsorption isotherm curve, the resulting biochar was classified into adsorption isotherm type I, which offers a microporous structure. When viewed from the pore shape, based on the isotherm adsorption-desorption hysteresis loop curve, the resulting biochar belongs to the H4 type (IUPAC/de Boer classification), which has narrow slit pores. Figure 10b shows the pore size distribution and cumulative volume of the pores in biochar. The figure shows that biochar has a limited pore size distribution range, with the dominant pore size in the field of 0 to 3 nm with a pore size distribution peak of 1.8 to 2 nm. The biochar product has a surface area of 0.3899 $m^2/g$.

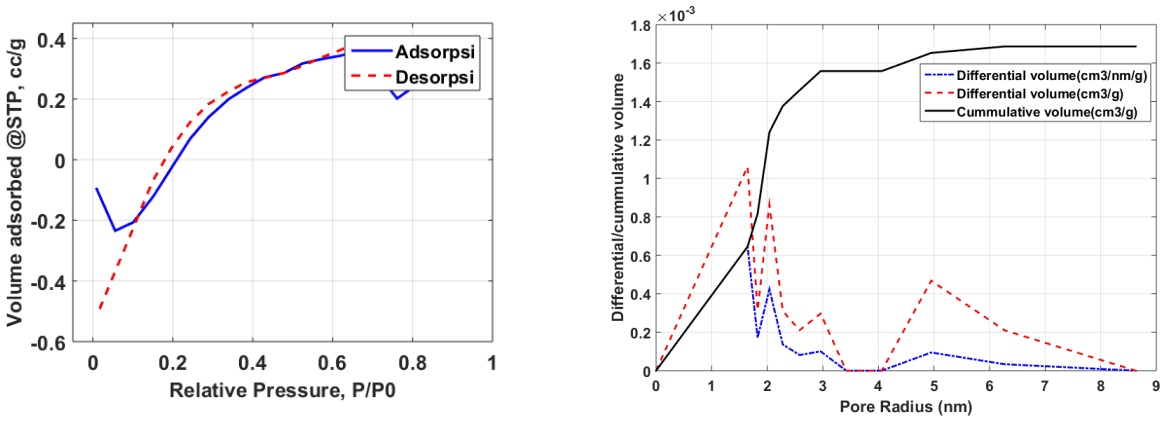


**Fig. 10.** Results of biochar analysis, a) the curve of isotherm adsorption-desorption, b) the curve of pore size distribution.

Table 3 shows the characteristics of biochar at the optimum pyrolysis temperature. From the table, it can be seen that biochar is included in the microporous material. As a microporous material, biochar from palm shell pyrolysis is weak when used as a catalyst for the cracking process because the small pore size does not allow long-chain hydrocarbon compounds to be adsorbed into the pores, thereby reducing conversion. Likewise, catalysts with microporous sizes are very quickly deactivated due to coking [51].

**Table 3**. Biochar characteristic at pyrolysis temperature of 550 ℃

| Parameters | Value |
|---|---|
| Surface Area ($m^2/g$) | 0.389946 |
| Mean Pore Size (nm) | 1.89417 |
| Total Pore Volume (cc/g) | 0.000369312 |

### *3.4. Characteristics of Gas Product*

The gas product at various non-catalytic and catalytic temperatures is shown in Figure 11. Figure 11 shows that high temperature increases the concentration of gaseous components. The gas products from palm shell pyrolysis consist of methane ($CH_4$) and carbon dioxide ($CO_2$). This differs from other literature, which states that pyrolysis gas consists of $H_2$, CO, $CH_4$, and $CO_2$ [14], [52]. Akubo et al. noted that the use of $Ni/Al_2O_3$ catalyst in pyrolysis of palm shells produced CO, $H_2$, $CO_2$, and $CH_4$ with volume percent respectively of 21.79%, 57.36%, 18.49%, and 2.27% [53]. The undetectable $H_2$ component is probably caused by methanation, hydrogenation, and dehydration reactions that convert hydrogen into alkanes and water or by the consumption of $H_2$ in the hydrocracking or hydrodeoxygenation processes.

Meanwhile, the undetected CO is probably caused by the methanation reaction, which converts CO into $CH_4$ and $H_2O$. $CH_4$ content is higher than $CO_2$. This may be due to the methanation process, which converts CO and $CO_2$ to $CH_4$. $Ni/Al_2O_3$ catalyst produces lower $CH_4$ and $CO_2$ than non-catalytic. $Ni/Al_2O_3$ catalyst is an effective metal catalyst for steam reforming, which converts $CH_4$ into CO and $H_2$. It is also effective for dry reforming, which converts $CH_4$ and $CO_2$ into CO and $H_2$ [54]. The high $CH_4$ and low $CO_2$ content indicate the potential of the pyrolysis process to produce biogas.

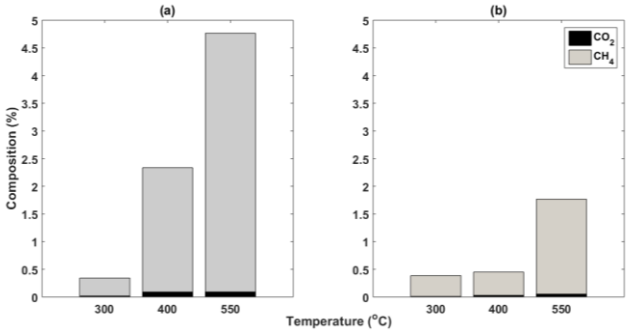


**Fig. 11.** Effluent gas composition.

## 4. Conclusion

Palm shell pyrolysis has the potential to be developed into valuable products as biofuels or chemicals. The experiment using a fixed bed reactor showed that the temperature increase does not significantly impact the rise in HHV and decrease of O/C and oxygenate content. Meanwhile, using a catalyst increases the HHV by 1.96%, reduces the O/C by 16.25%, and reduces the oxygenate content by 12.73%. Phenolic and fatty acid components are significant in palm shell bio-oil. Palm shell pyrolysis produces phenolic components as the primary value-added chemicals. $Ni/Al_2O_3$ catalyst has high selectivity to phenol, aliphatic hydrocarbons, and aldehydes. The gas product was dominated by methane ($CH_4$). $Ni/Al_2O_3$ catalyst is effective for steam and dry reforming process. The biochar product was classified into a microporous structure with a narrow slit pore, a mean pore diameter of 1.89 nm, and a surface area of 0.3899 $m^2/g$.

**Acknowledgments**

Financial support for this study was provided by the "Penelitian Dasar (PD)" scheme through the Research Grant from "Institute for Research and Community Service Universitas Ahmad Dahlan" for the Fiscal Year 2022, Number PD-072/SP3/LPPM-UAD/VII/2022.

**References**

[1] BPS, "Indonesian Oil Palm Statistics 2019," Badan Pus. Stat., p. 137, 2020.

[2] B. Subiyanto, H. Basri, L. N. Sari, and Y. Rosalita, "Chemical Components of Oil Palm ( Elaeis guineensis Jacq .) Shell and Its Effect on Light Concrete Performance," J. Trop. Wood Sci. Technol., Vol. 5, No. 4, 2007.

[3] J. P. Susanto, A. D. Santoso, and N. Suwedi, "Palm Solid Wastes Potential Calculation for Renewable Energy with LCA Method," J. Teknol. Lingkung., Vol. 18, No. 2, pp. 165–172, 2017.

[4] M. Van de Velden, J. Baeyens, A. Brems, B. Janssens, and R. Dewil, "Fundamentals, kinetics and endothermicity of the biomass pyrolysis reaction," Renew. Energy, Vol. 35, No. 1, pp. 232–242, 2010, DOI: 10.1016/j.renene.2009.04.019.

[5] T. Damartzis and A. Zabaniotou, "Thermochemical conversion of biomass to second generation biofuels through integrated process design-A review," Renew. Sustain. Energy Rev., Vol. 15, No. 1, pp. 366–378, 2011, DOI: 10.1016/j.rser.2010.08.003.

[6] V. K. Tyagi, L. A. Fdez-Güelfo, Y. Zhou, C. J. Álvarez-Gallego, L. I. R. Garcia, and W. J. Ng, "Anaerobic co-digestion of organic fraction of municipal solid waste (OFMSW): Progress and challenges," Renew. Sustain. Energy Rev., Vol. 93, No. June 2017, pp. 380–399, 2018, DOI: 10.1016/j.rser.2018.05.051.

[7] T. Tomić, D. F. Dominković, A. Pfeifer, D. R. Schneider, A. S. Pedersen, and N. Duić, "Waste to energy plant operation under the influence of market and legislation conditioned changes," Energy, Vol. 137, pp. 1119–1129, 2017, DOI: 10.1016/j.energy.2017.04.080.

[8] S. Hosokai, K. Matsuoka, K. Kuramoto, and Y. Suzuki, "Estimation of thermodynamic properties of liquid fuel from biomass pyrolysis," 3rd Int. Conf. Renew. Energy Res. Appl. ICRERA 2014, vol. 5, pp. 728–731, 19-22 Oktober 2014.

[9] J. Pitoyo, T. Eka, and S. Jamilatun, "Bio-oil from Oil Palm Shell Pyrolysis as Renewable Energy : A Review," Chem. J. Tek. Kim., Vol. 9, No. 2, pp. 67–79, 2022, DOI: 10.26555/chemica.v9i2.22355.

[10] S. Jamilatun, J. Pitoyo, and M. Setyawan, "Technical , Economic , and Environmental Review of Waste to Energy Technologies from Municipal Solid Waste," J. Ilmu Lingkung., Vol. 21, No. 3, pp. 581–593, 2023, DOI: 10.14710/jil.21.3.581-593.

[11] L. M. Terry, C. Li, J. J. Chew, A. Aqsha, B. S. How, A. C. M. Loy, and B. L. F. Chin, "Bio-oil production from pyrolysis of oil palm biomass and the upgrading technologies: A review," Carbon Resour. Convers., Vol. 4, No. October, pp. 239–250, 2021, DOI: 10.1016/j.crcon.2021.10.002.

[12] B. Nyoni and S. Hlangothi, "Evaluating the Potential of Algal Pyrolysis Bio-Oil as a Low-Cost Biodiesel for use in Standby Generators for home Power Generation," Int. J. Smart grid, Vol. 12, No. V6i4, pp. 3–6, 2023, DOI: 10.20508/ijsmartgrid.v6i4.258.g248.

[13] S. Jamilatun, J. Pitoyo, S. Amelia, A. Ma, D. C. Hakika, and I. Mufandi, "Experimental Study on The Characterization of Pyrolysis Products from Bagasse (Saccharum Officinarum L .) : Bio-oil , Biochar , and Gas Products," Indones. J. Sci. Technol., Vol. 7, No. 3, pp. 565–582, 2022, DOI: 10.17509/ijost.v7i3.51566.

[14] V. Han-U-Domlarpyos, P. Kuchonthara, P. Reubroycharoen, and N. Hinchiranan, "Quality improvement of oil palm shell-derived pyrolysis oil via catalytic deoxygenation over NiMoS/γ-Al2O3," Fuel, Vol. 143, pp. 512–518, 2015, DOI: 10.1016/j.fuel.2014.11.068.

[15] J. E. Omoriyekomwan, A. Tahmasebi, and J. Yu, "Production of phenol-rich bio-oil during catalytic fixed-bed and microwave pyrolysis of palm kernel shell," Bioresour. Technol., Vol. 207, pp. 188–196, May 2016, DOI: 10.1016/j.biortech.2016.02.002.

[16] G. Chang, P. Shi, Y. Guo, L. Wang, C. Wang, and Q. Guo, "Enhanced pyrolysis of palm kernel shell wastes to bio-based chemicals and syngas using red mud as an additive," J. Clean. Prod., Vol. 272, p. 122847, 2020, DOI: 10.1016/j.jclepro.2020.122847.

[17] Q. Niu, J. Wang, S. He, and Y. Zhu, "Exploring catalytic pyrolysis of Palm Shell over HZSM-5 by gas Chromatography/mass spectrometry and photoionization mass spectrometry," J. Anal. Appl. Pyrolysis, Vol. 152, No. October, p. 104946, 2020, DOI: 10.1016/j.jaap.2020.104946.

[18] S. W. Kim, B. S. Koo, and D. H. Lee, "Catalytic pyrolysis of palm kernel shell waste in a fluidized bed," Bioresour. Technol., Vol. 167, pp. 425–432, 2014, DOI: 10.1016/j.biortech.2014.06.050.

[19] F. Abnisa, W. M. A. W. Daud, W. N. W. Husin, and J. N. Sahu, "Utilization possibilities of palm shell as a source of biomass energy in Malaysia by producing bio-oil in pyrolysis process," Biomass and Bioenergy, Vol. 35, No. 5, pp. 1863–1872, 2011, DOI: 10.1016/j.biombioe.2011.01.033.

[20] S. Jamilatun, M. Aziz, and J. Pitoyo, "Multi-Distributed Activation Energy Model for Pyrolysis of Sugarcane Bagasse : Modelling Strategy and Thermodynamic Characterization," Indones. J. Sci. Technol., Vol. 8, No. 3, pp. 413–428, 2023, DOI: 10.17509/ijost.v8i3.60175.

[21] H. Yang, R. Yan, H. Chen, D. H. Lee, and C. Zheng, "Characteristics of hemicellulose, cellulose and lignin

pyrolysis," Fuel, Vol. 86, No. 12–13, pp. 1781–1788, 2007, DOI: 10.1016/j.fuel.2006.12.013.

[22] T. Aysu, M. M. Maroto-Valer, and A. Sanna, "Ceria promoted deoxygenation and denitrogenation of Thalassiosira weissflogii and its model compounds by catalytic in-situ pyrolysis," Bioresour. Technol., Vol. 208, pp. 140–148, 2016, DOI: 10.1016/j.biortech.2016.02.050.

[23] R. R. Davda, J. W. Shabaker, G. W. Huber, R. D. Cortright, and J. A. Dumesic, "A review of catalytic issues and process conditions for renewable hydrogen and alkanes by aqueous-phase reforming of oxygenated hydrocarbons over supported metal catalysts," Applied Catalysis B: Environmental, Vol. 56, pp. 171–186, 2005, DOI: 10.1016/j.apcatb.2004.04.027.

[24] M. M. Khader, M. J. A.-. Marri, S. Ali, and A. G. Abdelmoneim, "Catalytic evaluation of Ni-based nano-catalysts in dry reformation of methane," IEEE 17th International Conference on Nanotechnology (IEEE-NANO), 2017, pp. 1051–1055. DOI: 10.1109/NANO.2017.8117488, 25-28 July 2017.

[25] W. Ma, L. Han, L. Zhang, and W. Lu, "Thermal-reforming of toluene over core-shell Ni/γ-Al2O3 catalysts," International Conference on Materials for Renewable Energy and Environment, 2013, pp. 492–495. DOI: 10.1109/ICMREE.2013.6893718, 19-21 August 2013.

[26] H. Yang, S. Li, B. Liu, and Y. Chen, "Hemicellulose pyrolysis mechanism based on functional group evolutions by two-dimensional perturbation correlation infrared spectroscopy," Fuel, Vol. 267, No. February, p. 117302, 2020, DOI: 10.1016/j.fuel.2020.117302.

[27] M. Faisal, A. Gani, F. Mulana, H. Desvita, and S. Kamaruzzaman, "Effects of pyrolysis temperature on the composition of liquid smoke derived from oil palm empty fruit bunches," Rasayan J. Chem., Vol. 13, No. 1, pp. 514–520, Jan. 2020, DOI: 10.31788/RJC.2020.1315507.

[28] T. Kan, V. Strezov, and T. J. Evans, "Lignocellulosic biomass pyrolysis: A review of product properties and effects of pyrolysis parameters," Renew. Sustain. Energy Rev., Vol. 57, pp. 1126–1140, 2016, DOI: 10.1016/j.rser.2015.12.185.

[29] N. Nastasiienko, T. Kulik, B. Palianytsia, J. Laskin, and T. Cherniavska, "Catalytic Pyrolysis of Lignin Model Compounds ( Pyrocatechol , Guaiacol , Vanillic and Ferulic Acids ) over Nanoceria Catalyst for Biomass Conversion," Appl. Sci., Vol. 11, No. 16, pp. 7205, 2021. DOI: 10.3390/app11167205

[30] S. D. Stefanidis, K. G. Kalogiannis, E. F. Iliopoulou, C. M. Michailof, P. A. Pilavachi, and A. A. Lappas, "A study of lignocellulosic biomass pyrolysis via the pyrolysis of cellulose, hemicellulose and lignin," J. Anal. Appl. Pyrolysis, Vol. 105, pp. 143–150, 2014, DOI: 10.1016/j.jaap.2013.10.013.

[31] R. J. Evans and T. A. Milne, "Molecular characterization of the pyrolysis of biomass," Energy & Fuels, Vol. 1, No. 2, pp. 123–137, Mar. 1987, DOI: 10.1021/ef00002a001.

[32] M. Hu, M. Laghari, B. Cui, B. Xiao, B. Zhang, and D. Guo, "Catalytic cracking of biomass tar over char supported nickel catalyst," Energy, Vol. 145, pp. 228–237, 2018, DOI: 10.1016/j.energy.2017.12.096.

[33] S. Jamilatun, D. C. Hakika, and J. Pitoyo, "Reaction kinetics of Components of Ex-Situ Slow Pyrolysis of Spirulina Platensis Residue with Silica- alumina Catalyst Through 5-Lump Model," Int. J. Renew. Energy Res., Vol. 12, No. 3, pp. 1372–1382, 2022, DOI: 10.20508/ijrer.v12i3.13159.g8533.

[34] M. Balat, "Mechanisms of Thermochemical Biomass Conversion Processes. Part 3: Reactions of Liquefaction," Energy Sources Part A-recovery Util. Environ. Eff., Vol. 30, pp. 649–659, Mar. 2008, DOI: 10.1080/10407780600817592.

[35] C. A. Fisk, T. Morgan, Y. Ji, M. Crocker, C. Crofcheck, and S. A. Lewis, "Bio-oil upgrading over platinum catalysts using in situ generated hydrogen," Applied Catalysis A: General , Vol. 358, pp. 150–156, 2009, DOI: 10.1016/j.apcata.2009.02.006.

[36] F. N. Ani, "Oil palm shell as a source of phenol," J. Oil Palm Res., Vol. 12, No. 1, pp. 86–94, 2000.

[37] G. Chang, P. Miao, H. Wang, L. Wang, X. Hu, and Q. Guo, "A synergistic e ff ect during the co-pyrolysis of Nannochloropsis sp . and palm kernel shell for aromatic hydrocarbon production," Energy Convers. Manag., Vol. 173, No. April, pp. 545–554, 2018, DOI: 10.1016/j.enconman.2018.08.003.

[38] Yogalakshmi, D. Poornima, Sivashanmugam, and Kavitha, "Lignocellulosic biomass-based pyrolysis: A comprehensive review," Chemosphere, Vol. 286, No. P2, p. 131824, 2022, DOI: 10.1016/j.chemosphere.2021.131824.

[39] B. Yu, C. Li, L. Gu, and L. Zhang, "Eugenol protects against Aspergillus fumigatus keratitis by inhibiting inflammatory response and reducing fungal load," Eur. J. Pharmacol., Vol. 924, Jun. 2022, DOI: 10.1016/j.ejphar.2022.174955.

[40] G. Chang, P. Miao, X. Yan, G. Wang, and Q. Guo, "Phenol preparation from catalytic pyrolysis of palm kernel shell at low temperatures," Bioresour. Technol., Vol. 253, pp. 214–219, Apr. 2018, DOI: 10.1016/j.biortech.2017.12.084.

[41] G. Widiyarti, J. Abbas, and Y. Anita, "Biotransformation and cytotoxic activity of guaiacol dimer," Indones. J. Chem., Vol. 14, No. 2, pp. 179–184, 2014, DOI: 10.22146/ijc.21256.

[42] N. Li, J. Su, H. Wang, and A. Cavaco-Paulo, "Production of antimicrobial powders of guaiacol oligomers by a laccase-catalyzed synthesis reaction," Process Biochem., Vol. 111, pp. 213–220, Dec. 2021, DOI: 10.1016/j.procbio.2021.07.018.

[43] K. Soongprasit, V. Sricharoenchaikul, and D. Atong, "Phenol-derived products from fast pyrolysis of organosolv lignin," Energy Reports, Vol. 6, pp. 151–167, Nov. 2020, DOI: 10.1016/j.egyr.2020.08.040.

[44] H. Li, L. Lin, Y. Feng, and M. Zhao, "Enrichment of antioxidants from soy sauce using macroporous resin and identification of 4-ethylguaiacol, catechol, daidzein, and 4-ethylphenol as key small molecule antioxidants in soy sauce," Food Chem., Vol. 240, pp. 885–892, Feb. 2018, DOI: 10.1016/j.foodchem.2017.08.001.

[45] E. Aliu, A. Hart, and J. Wood, "Mild-Temperature hydrodeoxygenation of vanillin a typical bio-oil model compound to Creosol a potential future biofuel," Catal. Today, Vol. 379, pp. 70–79, Nov. 2021, DOI: 10.1016/j.cattod.2020.05.066.

[46] A. M. Api, D. Belsito, D. Botelho, and M. Bruze, "RIFM fragrance ingredient safety assessment, 2,6-dimethoxyphenol, CAS Registry Number 91-10-1," Food and Chemical Toxicology, Vol. 165. Elsevier Ltd, Jul. 01, 2022. DOI: 10.1016/j.fct.2022.113092.

[47] B. Irem and O. Korkmaz, "The anti-campylobacter activity of eugenol and its potential for poultry meat safety : A review," Vol. 394, No. June, 2022, DOI: 10.1016/j.foodchem.2022.133519.

[48] M. Najib and M. N. Islam, "Slow pyrolysis system of agricultural solid waste for bio-char," 7th Brunei International Conference on Engineering and Technology 2018 (BICET 2018), 2018, pp. 1–4. DOI: 10.1049/cp.2018.1571, 12-14 November 2018.

[49] S. Jamilatun, S. Amelia, J. Pitoyo, and A. Ma'arif, "Preparation and Characteristics of Effective Biochar Derived from Sugarcane Bagasse as Adsorbent," Int. J. Renew. Energy Res., Vol. 13, No. 2, 2023, DOI: 10.20508/ijrer.v13i2.13719.g8737.

[50] N. S. Lazarenko, N. I. Lapekin, A. A. Shestakov, and A. G. Bannov, "Directed Synthesis of Carbonized Materials from Agroindustrial Wastes for Supercapacitors," IEEE 23rd International Conference of Young Professionals in Electron Devices and Materials (EDM), 2022, pp. 71–74. DOI: 10.1109/EDM55285.2022.9855170, 30 June 2022 - 04 July 2022.

[51] Z. A. Alothman, "A Review: Fundamental Aspects of Silicate Mesoporous Materials," Materials, Vol. 5, No. 12, pp.2874–2902. DOI: 10.3390/ma5122874.

[52] K. Akubo, M. A. Nahil, and P. T. Williams, "Pyrolysis-catalytic steam reforming of agricultural biomass wastes and biomass components for production of hydrogen / syngas," J. Energy Inst., Vol. 92, No. 6, pp. 1987–1996, 2019, DOI: 10.1016/j.joei.2018.10.013.

[53] D. Song, U. Jung, H. B. Im, K. B. Lee, and K. Y. Koo, "Dry Reforming of Methane over Ni-Ru/MgAl2O4 Catalyst with High Coke Resistance for Syngas Production," 5th International Conference on Smart and Sustainable Technologies (SpliTech), 2020, pp. 1–4. DOI: 10.23919/SpliTech49282.2020.9243723, 23-26 September 2020.

[54] C.-H. Liao and R.-F. Horng, "Study on the operating range for syngas production by oxidation dry reforming of biogas," International Conference on Applied System Innovation (ICASI), 2016, pp. 1–4. DOI: 10.1109/ICASI.2016.7539748, May 2016.